Trans Indian Inst Met (2015) 68(5):851–857
DOI 10.1007/s12666-015-0519-7

TECHNICAL PAPER

TP 2910

Effect of Film Formation Potential on the Electrochemical Behavior of the Passive Films Formed on Zinc in 0.01 M NaOH

Arash Fattah-alhosseini · Mahyar Mirshekari

Received: 21 November 2014 / Accepted: 22 January 2015 / Published online: 28 March 2015

Abstract This work focuses on the electrochemical behavior of zinc in 0.01 M NaOH solution. The results include determination of the semiconductor behavior of the passive film, as well as the estimation of its thickness as a function of the film formation potential. Mott–Schottky analysis revealed that the passive films displayed n-type semiconductive characteristics, where the oxygen vacancies and interstitials preponderated. Moreover, it was shown that the calculated donor density increases with increasing formation potential. Electrochemical impedance spectroscopy results indicated that the thickness of the passive film was increased linearly with increasing formation potential. The results showed that increasing the formation potential offer worse conditions for forming the passive films with lower protection behavior, due to the growth of a much thicker and higher defective films.

Keywords Zinc · EIS · Mott–Schottky · Passive films · Formation potential

1 Introduction

Mott–Schottky analysis is extensively used to revisit the semiconducting behaviors of the passive films formed on pure metals, such as iron [1–3], nickel [4–6], titanium [7–9], chromium [10], aluminum [11], cobalt [12], zinc [13] and tungsten [14]. Moreover, point defect model (PDM) [15–18] is based on the assumption that the growth of the passive film involves the migration of the point defects in the passive film. Therefore, by using Mott-Schottky analysis in conjunction with the PDM, the dopant density and diffusivity for the passive film formed on pure metals [19–21] can be easily determined.

According to the potential–pH diagram for zinc and water, this metal corrodes in acidic solutions. Indeed, the principal drawback of zinc and its alloys are the low corrosion resistance in acidic solutions, which is generally much lower when compared to many other metals. Nevertheless, at high pH (slightly and strong alkaline solutions), in the region identified as passive, the surface film formed on zinc is protective. In the last decade, many studies investigated the passivation and electrochemical behavior of zinc in strong alkaline solution. Indeed, these studies are related to battery applications and deal with the problem of passivation for alkaline batteries under a high discharge rate [13].

Mott–Schottky analysis has been widely employed to determine the dopant levels of the passive film formed on most pure metals, such as Fe [3], W [14] and Nb [22]. However, little information about the semiconducting behavior of pure zinc in alkaline solutions is available [23–26]. Scholl et al. [27] investigated the photocurrent plots of the passive films formed on zinc in KOH solutions and showed that the passive films exhibited semiconducting properties. Also, Macdonald et al. [28] and Shang et al. [13] showed that the passive films formed on zinc are highly defective and exhibit n-type semiconductive characteristics.

Despite the extensive works published on the passivity of zinc in alkaline solutions [13, 23–32], little information about the effect of the formation potential on the semiconductive behavior of the passive film formed on this metal is available. In this work, Mott–Schottky analysis and EIS measurements of pure zinc in alkaline solution

A. Fattah-alhosseini (✉) · M. Mirshekari
Faculty of Engineering, Bu-Ali Sina University, Hamedan 65178-38695, Iran
e-mail: a.fattah@basu.ac.ir; arash.fattah@gmail.com

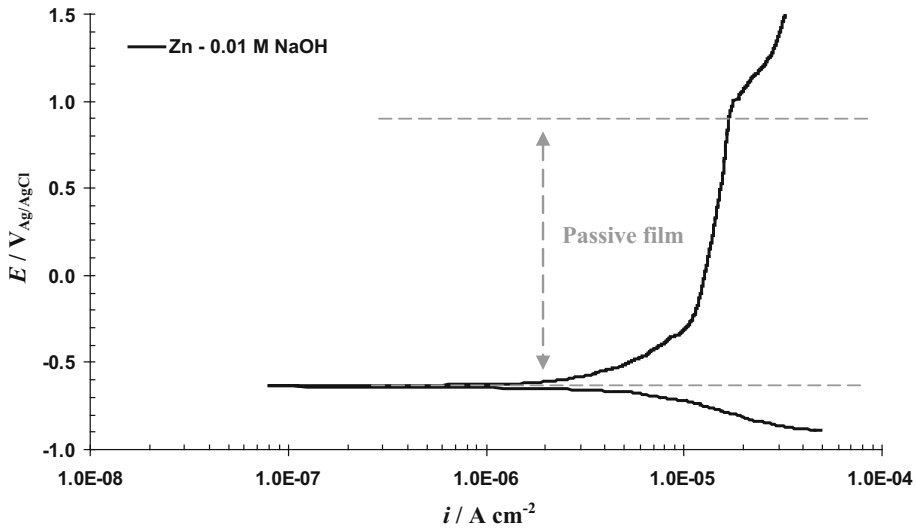

Fig. 1 Polarization curve of zinc in 0.01 M NaOH solution in the anodic direction at 1 mV/s

(0.01 M NaOH) have been done to clarify the semiconductor behavior of the passive film.

2 Experimental procedures

Specimens were fabricated from a thick plate of pure zinc. All samples were ground to 2,500 grit and cleaned by deionized water prior to tests. All the electrochemical measurements were done in a conventional three-electrode flat cell under aerated conditions in 0.01 M NaOH solution at 25 ± 1 °C by using μAutolab Type III/FRA2 system controlled by a personal computer. The counter electrode was a Pt plate, while the reference electrode was Ag/AgCl saturated in KCl. The electrochemical measurements were performed in the following sequence:

(a) Potentiodynamic polarization curve was measured potentiodynamically at a scan rate of 1 mV/s starting from −0.25 $V_{Ag/AgCl}$ (vs. E_{corr}) to 1.5 $V_{Ag/AgCl}$.
(b) Five formation potentials (0.1, 0.3, 0.5, 0.7 and 0.9 $V_{Ag/AgCl}$) within the passive region were chosen for EIS and Mott–Schottky measurements. Passive films were grown at each potential to ensure that the system was in steady-state. After each passive film growth period, EIS and Mott–Schottky measurements were performed. The impedance spectra were measured in a frequency range of 100 kHz–100 mHz at an AC amplitude of 10 mV (rms) [13]. For the EIS data modeling and curve-fitting method, the NOVA impedance software was used. Mott–Schottky analyses were done by measuring the frequency response at 1 kHz during a 25 mV/s negative potential scan from each selected potential to −1.0 $V_{Ag/AgCl}$.

3 Results and Discussion

3.1 Polarization Measurement

Figure 1 shows the potentiodynamic polarization curve of zinc in 0.01 M NaOH. According to this figure, the current density was found to increase slowly with potential during the early stage of passivation and no obvious current peak was observed.

It is observed that the passive potential range is extending from the corrosion potential (−0.6 $V_{Ag/AgCl}$) to 0.9 $V_{Ag/AgCl}$. This metal in alkaline solutions exhibits the same curve shapes [29], where the current changes smoothly and linearly around the rest potential manifesting cathodic and anodic Tafel behavior.

3.2 Mott–Schottky Analysis

Figure 2 shows the Mott-Schottky plots of zinc in 0.01 M NaOH solution at selected formation potentials. As can be seen, C^{-2} clearly decrease with increasing formation potential. In this Figure, the positive slopes are attributed to n-type behavior. Also, in the potential range of around -0.6–0.9 $V_{Ag/AgCl}$ no evidence for p-type behavior was observed, indicating that cation vacancies do not have any significant population density in the passive film.

Similar Mott–Schottky plots for zinc in 0.1 M NaOH solution have been reported by Shang et al. [13]. According to Eq. (1), the donor density (N_D, cm^{-3}) can be calculated from the slope of the experimental $1/C^2$ versus E plots [19–21]:

$$\frac{1}{C_{SC}^2} = \frac{2}{\varepsilon\varepsilon_0 e N_D}\left(E - E_{FB} - \frac{k_B T}{q}\right) \text{for } n-\text{type semiconductor} \quad (1)$$

where e is the electron charge, ε is the dielectric constant of the passive film ($\varepsilon = 8.5$ for ZnO [13]), K_B is the Boltzmann constant, T is the absolute temperature and E_{FB} is the flat band potential. From Eq. (1) Flat band potential can be determined from the extrapolation of the linear portion to $C^{-2} = 0$ [32]. The flat band potential estimated from Fig. 2 is plotted as a function of formation potential in Fig. 3. The values agree well with the literature data [24, 31]. The calculated flat band potential for passive zinc was found to vary with formation potential in a manner that is observed for n-type passive films formed on iron and tungsten (E_{FB} decreases with increasing film formation potential) [4].

Figure 4 shows the calculated donor density of the passive film formed on zinc in 0.01 M NaOH at selected formation potentials. The orders of magnitude are around 10^{20} cm^{-3} and increases with the formation potential. The values are comparable to the calculated donor density of the passive film formed on zinc and its alloys in alkaline solutions [24, 26, 28, 30, 31].

3.3 General Discussion

In Fig. 2, the positive slopes are attributed to n-type behavior. Also, according to Fig. 4, the donor density increases with the formation potential. Indeed, the changes in the donor density are related to the non-stoichiometry defects in the passive films. Moreover, this tendency is due to the charge neutrality of the passive films.

PDM presupposes that passive films are bilayer structures comprising a defective barrier layer that grows into

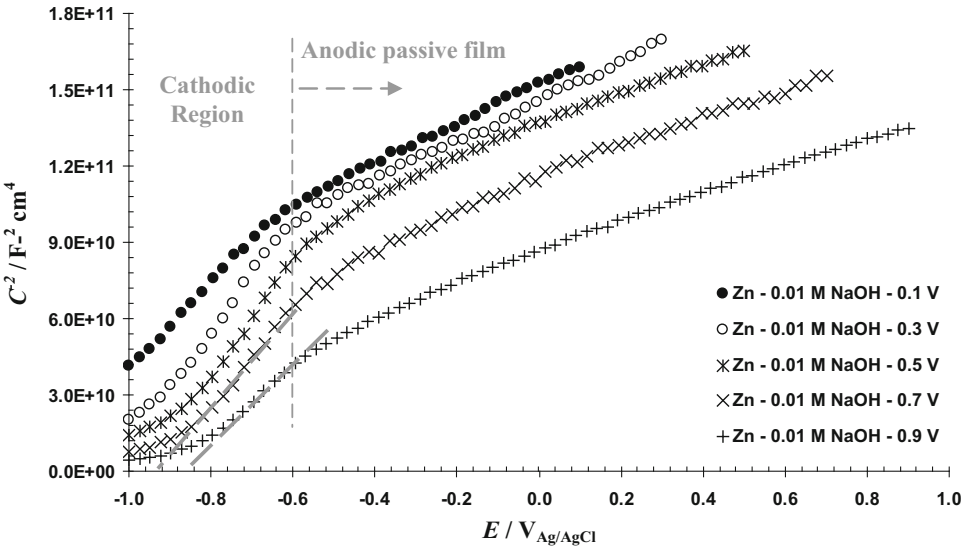

Fig. 2 Mott-Schottky plots of passive film formed at different formation potential on zinc in 0.01 M NaOH solution

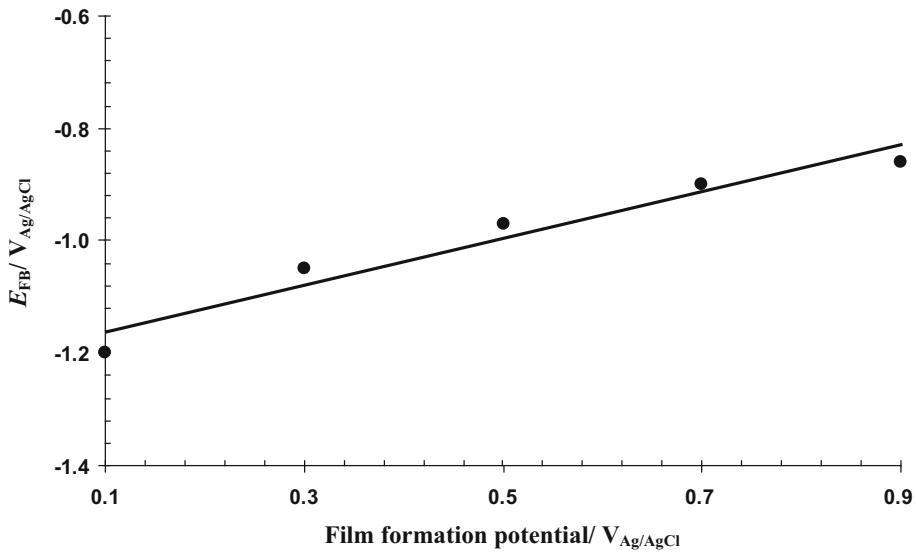

Fig. 3 Flat band potential versus formation potential for passive zinc in 0.01 M NaOH solution

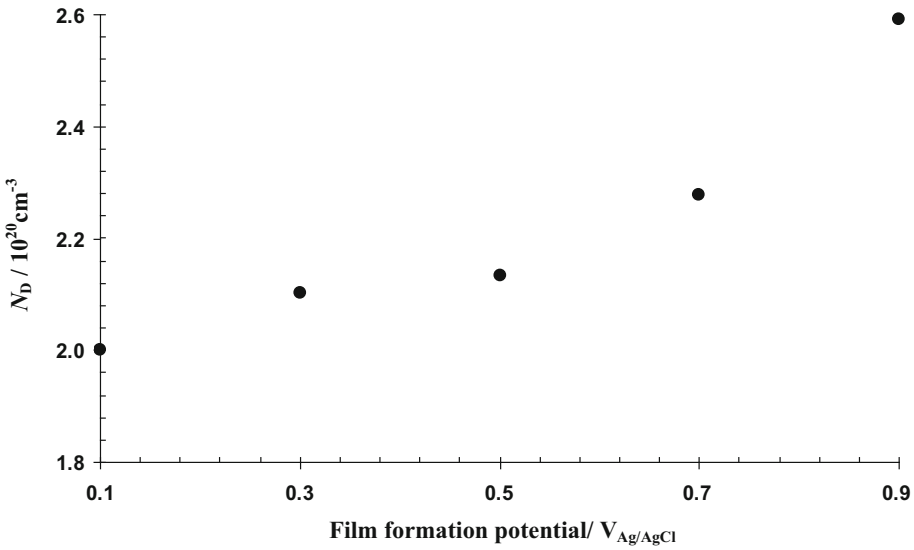

Fig. 4 Donor densities of the passive films formed on zinc in 0.01 M NaOH solution as a function of film formation potential

the metal and an outer layer that forms via the hydrolysis of cations transmitted through the barrier layer and the subsequent precipitation of a hydroxide, or oxide, depending upon the formation conditions. Also, PDM assumes that the point defects present are, in general, cation vacancies ($V_M^{\chi'}$), oxygen vacancies ($V_O^{\cdot\cdot}$), and cation interstitials ($M_i^{\chi+}$), as designated by the Kroger-Vink notation. Cation vacancies are electron acceptors, thereby doping the barrier layer p-type, whereas oxygen vacancies and cation interstitials are electron donors, resulting in n-type doping [13–16].

X-ray photoemission spectroscopy studies on zinc and its alloys show the existence of the barrier layer and outer layer. The inner layer involves the two main point defects of ZnO namely, zinc cation interstitials and oxygen vacancies and the outer precipitated layer forms by the hydrolysis of ejected cations. The nature of outer layer (and hence the type of precipitated oxide) has a strong dependence on the solution pH. In the pH range 12–13, thermodynamic predictions reveal that zinc cation in solution could form either ZnO, $Zn(OH)_2$, $Zn(OH)_3^-$ or $Zn(OH)_4^{2-}$, each possibly altering the nature of the precipitated layer [29]. Therefore based on the n-type behavior of the passive film formed on zinc in 0.01 M NaOH, the dominant point defects must be oxygen vacancies ($V_O^{\cdot\cdot}$) and zinc cation interstitials (Zn_i^{n+}). Figure 5 shows the PDM of zinc passivation in alkaline solutions. As the passive films compose of zinc cation interstitials (Zn_i^{n+}), the tendency of oxidation reaction of Zn_i^+ to Zn_i^{2+} increases with the increase of formation potential. When the substitution of Zn_i^+ by Zn_i^{2+} develops gradually, the films produces an ionic species (Zn_{Zn}^+) that has a charge of +1. Considering the charge neutrality in the films, the increment density of oxygen vacancies ($V_O^{\cdot\cdot}$) should be produced. Therefore, it is concluded

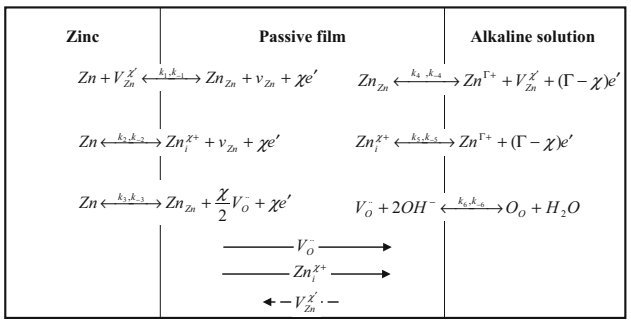

Fig. 5 PDM of passivation of zinc in alkaline solutions. Zn_{Zn} = zinc cation on the zinc sublattice and O_O = oxygen anion on the oxygen sublattice

that the oxygen vacancies and zinc cation interstitials increase with increasing formation potential.

3.4 EIS measurements

The EIS response of zinc in 0.01 M NaOH solution at selected formation potentials are presented as Nyquist, Bode, and Bode-phase plots in Fig. 6. The Nyquist, Bode, and Bode-phase plots show a resistive behavior at high frequencies, but in the middle to low frequency range there was a marked capacitive response. Also in the Nyquist and Bode plots, there was a decrease of the low frequency impedance with the formation potentials.

The Bode-phase curves (Fig. 6(c)) show one time constant (only one maximum phase lag at the middle frequency range). The phase angles values (remained very close to 80°) revealed the formation and growth of a passive film. Similar plots for the EIS response of zinc in 0.1 M NaOH solution have been reported by Shang et al. [13].

Based on these results, the equivalent circuit shown in Fig. 7 was used to simulate the measured impedance data on zinc in 0.01 M NaOH solution. This equivalent circuit is composed of: R_s – solution resistance; Q_{pf} – constant phase element corresponding to the capacitance of the passive film; R_{pf} – resistance of the passive film [33, 34].

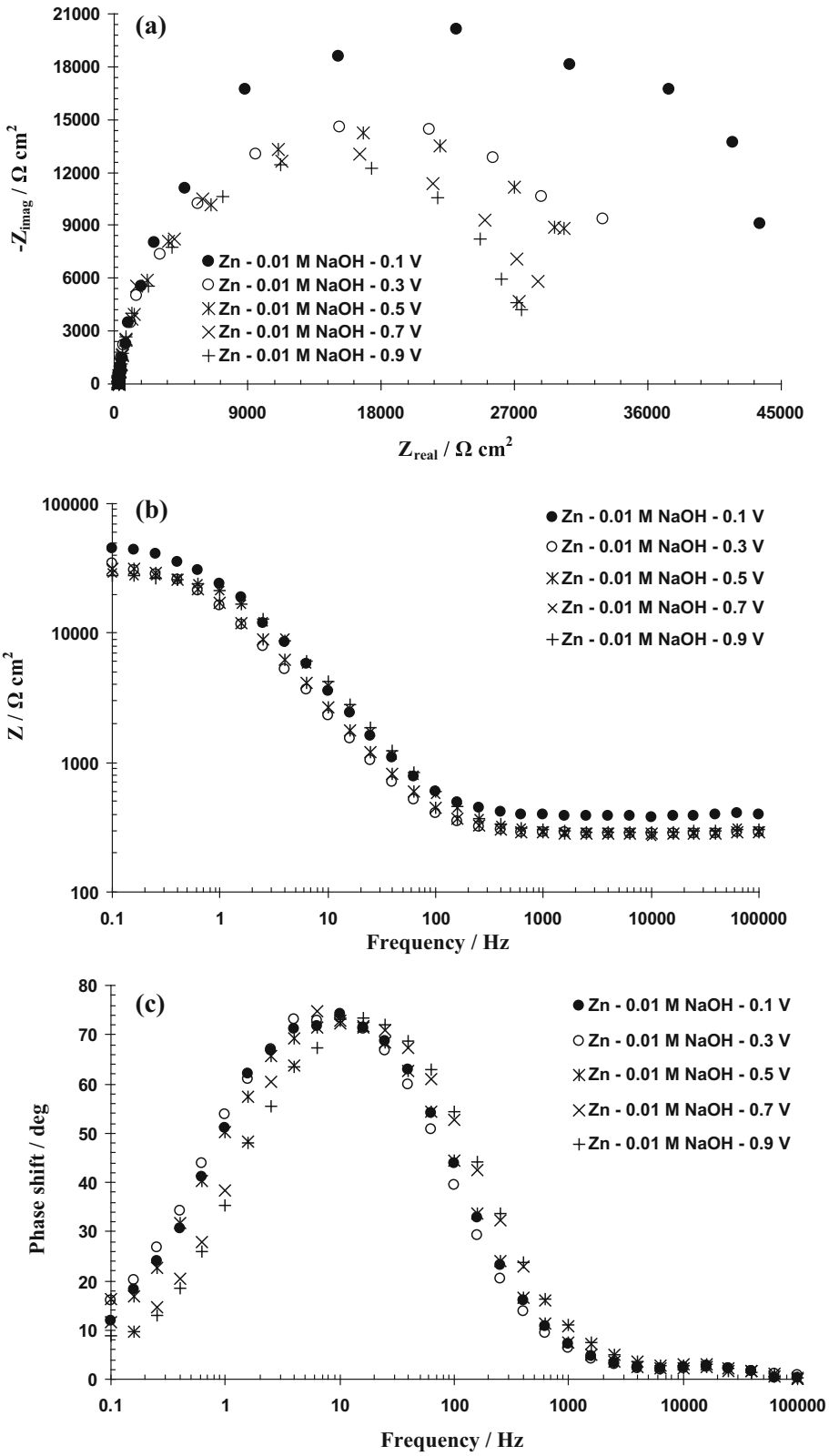

Fig. 6 **a** Nyquist, **b** Bode and (b) Bode-phase plots of zinc in 0.01 M NaOH solution measured at different formation potential

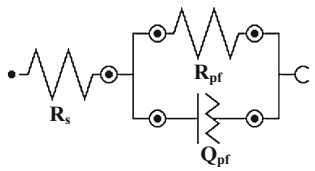

Fig. 7 The best equivalent circuit used to model the experimental EIS data [33, 34]

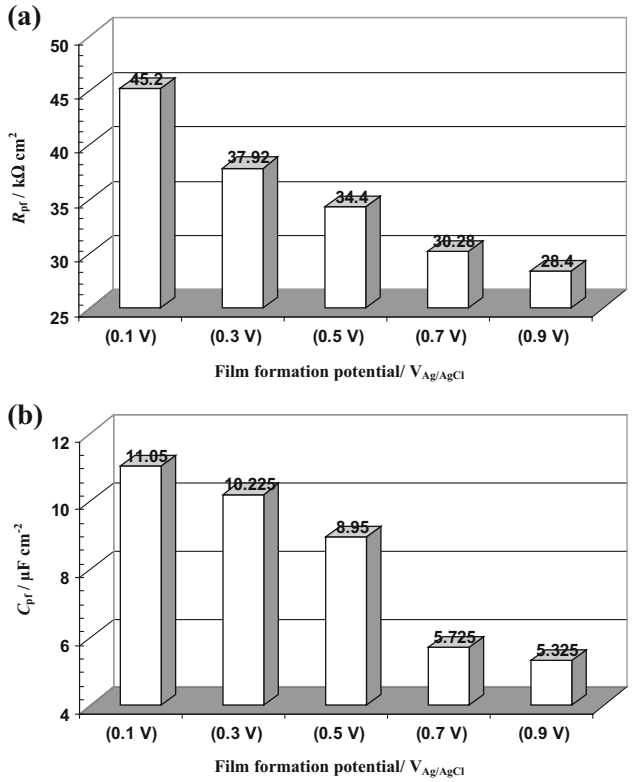

Fig. 8 Variation of the (a) resistance and (b) capacitance of the passive films formed on zinc in 0.01 M NaOH solution

The variation of the resistance and capacitance of the passive films formed on zinc in 0.01 M NaOH solution are illustrated in Fig. 8 (a) and (b), respectively. As can be seen, both resistance and capacitance of the passive films decrease with increase in formation potentials.

Figure 9 shows a linear relationship between the passive film thickness (d) and the formation potential. This relationship between the passive film thickness and the formation potential has been found earlier by Sikora et al. [16]. According to Eq. (2), the film thickness was determined from the capacitance measured at 1 kHz at each constant potential growth [21]:

$$d = \frac{\varepsilon\varepsilon_0 A}{C} \tag{2}$$

The calculated thickness ranges from about 1.147 nm at 0.1 $V_{Ag/AgCl}$ to 2.727 nm at 0.9 $V_{Ag/AgCl}$.

Therefore, it is concluded that increasing the formation potential offer worse conditions for forming the passive films with lower protection behavior, due to the growth of much thicker and higher defective films.

4 Conclusions

In this work, Mott–Schottky analysis and EIS measurements of pure zinc in 0.01 M NaOH solution have been done to clarify the semiconductor behavior of passive film. Conclusions drawn from the study are as follows

1. Mott–Schottky analysis revealed that the passive films displayed n-type semiconductive characteristics, where the oxygen vacancies and interstitials preponderated.
2. It was shown that the calculated donor density increases with increasing the formation potential.

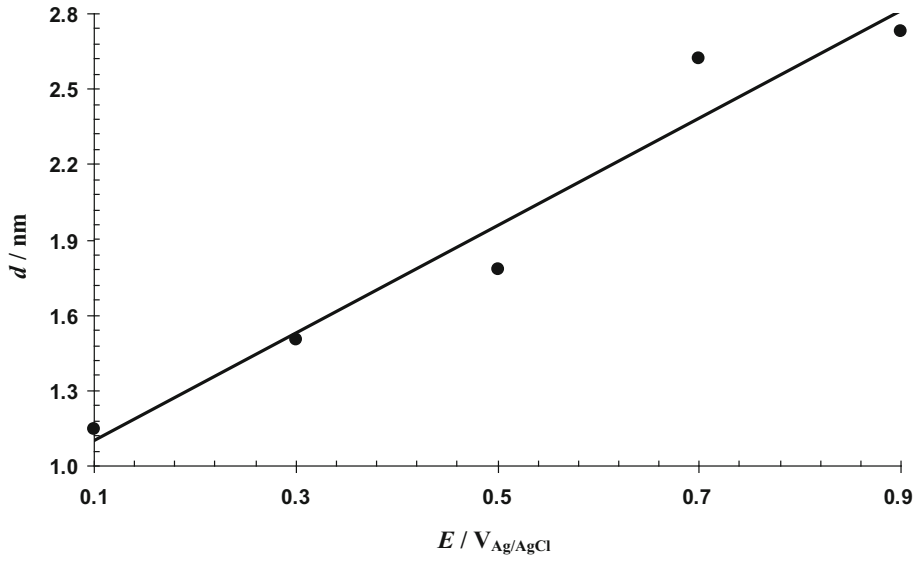

Fig. 9 Effect of the formation potential on the passive film thickness of zinc in 0.01 M NaOH solution

3. The Nyquist, Bode, and Bode-phase plots show a resistive behavior at high frequencies, but in the middle to low frequency range there was a marked capacitive response.
4. Also, the EIS results indicated that the thickness of the passive film was increased linearly with increasing formation potential.
5. The results showed that increasing the formation potential offers worse conditions for forming the passive films with lower protection behavior, due to the growth of much thicker and higher defective films.

References

1. Harrington S P, Wang F, and Devine T M, Electrochim Acta **55** (2010) 4092.
2. Wielant J, Goossens V, Hausbrand R, and Terryn H, Electrochim Acta **52** (2007) 7617.
3. Ahn S J, and Kwon H S, J Electroanal Chem **579** (2005) 311.
4. Sikora E, and Macdonald DD Electrochim Acta **48** (2002) 69.
5. Darowicki K, Krakowiak S, and Ślepski P, Electrochim Acta, **51** (2006) 2204.
6. Grubač Z, Petrović Ž, Katić J, Metikoš-Huković M, and Babić R, J Electroanal Chem **645** (2010) 87.
7. Schmidt AM, Azambuja DS, and Martini EMA, Corros Sci **48** (2006) 2901.
8. Jiang P, Liang J, and Lin C, Appl Surf Sci **280** (2013) 373.
9. Jiang Z, Dai X, and Middleton H, Mater Chem Phys **126** (2011) 859.
10. Kong D-S, Chen S-H, Wang C, and Yang, Corros Sci **45** (2003) 747.
11. Martin FJ, Cheek GT, Grady WEO, and Natishan PM, Corros Sci **47** (2005) 3187.
12. Pontinha M, Faty S, Walls MG, Ferreira MGS, and Da Cunha M, Corros Sci **48** (2006) 2971.
13. Shang X-L, Zhang B, Han E-H, and Ke W, Electrochim Acta **56** (2011) 1417.
14. Sikora J, Sikora E, and Macdonald DD, Electrochim Acta **45** (2000) 1875.
15. Zhang Y, Macdonald DD, Urquidi-Macdonald M, Engelhard GR, and Dooley RB, Corros Sci **48** (2006) 3812.
16. Sikora E, Sikora J, and Macdonald DD, Electrochim Acta 41 (1996) 783.
17. Macdonald DD, J Electrochem Soc**153** (2006) B213.
18. Macdonald DD, J Nucl Mater **379** (2008) 24.
19. Fattah-alhosseini A, Golozar MA, Saatchi A, and Raeissi K, Corros Sci **52** (2010) 205.
20. Fattah-alhosseini A, Soltani F, Shirsalimi F, Ezadi B, and Attarzadeh N, Corros Sci **53** (2011) 3186.
21. Fattah-alhosseini A, Saatchi A, Golozar MA, and Raeissi K, J Appl Electrochem **40** (2010) 457.
22. Li DG, Wang JD, and Chen DR, Electrochim Acta 60 (2012) 134.
23. Mishima H, de Mishima L, Santos E, De Pauli CP, Azumi K, and Sato N, Electrochim Acta **36** (1991) 1491.
24. Bohe A E, Vilche J R, Jüttner K, Lorenz W J, Kautek W, and Paatasch W, Corros Sci **32** (1991) 621.
25. Bohe AE, Vilche JR, Jüttner K, Lorenz WJ, and Paatsc W, Electrochimica Acta **34** (1989) 1443.
26. Vilche JR, Jüttner K, Lorenz WJ, Kautek W, Paatsch W, Dean MH, and Stimmin U, Corros Sci **31** (1990) 679.
27. Scholl P, Shan X, Bonham D, and Prentice G A, J Electrochem Soc **138** (1991) 895.
28. Macdonald D D, Ismail K M, and Sikora E, J Electrochem Soc **145** (1998) 3141.
29. Thomas S, Cole I S, Sridhar M, and Birbilis N, Electrochim Acta **97** (2013) 192.
30. Pech-Canul M A, Ramanauskas R, and Maldonado L, Elecfrochim Acta **42** (1997) 255.
31. Rudd A L, and Breslin C B, Electrochim Acta **45** (2000) 1571.
32. Gelderman K, Lee L, and Donne S W, J Chem Educ **84** (2007) 685.
33. El-Sayed A-R, Mohran H S, and Abdel-Lateef H M, Metall Mater Trans A **43** (2012) 619.
34. Fattah-alhosseini A, and Sabaghi Joni M, J Magnes Alloy **2** (2014) 175.